SET-UP DUE TO RANDOM WAVES: INFLUENCE OF THE DIRECTIONAL SPECTRUM

G Barbaro, **G Foti, G Malara,** Department of Mechanics and Materials, 'Mediterranea' University of Reggio Calabria, Italy

SUMMARY

The correct estimation of set-up is very important to evaluate coastal hazard and to design coastal structures. In this paper, we derived a mathematical expression for wave set-up in the context of random waves. The solution to this expression assumes straight, parallel depth contours and constant average flow parameters in the longshore direction. We then investigated the effect of different types of sea state taking account of different frequency spectrum and spreading function assumed in the expression on estimates of wave set-up. We found the set-up was highly influenced by the frequency spectrum used. Finally, we applied this expression to estimate set-up values at locations in Italy and in the United States using buoy data provided by ISPRA (Istituto Superiore per la Protezione e la Ricerca Ambientale) and NDBC (National Data Buoy Centre).

NOMENCLATURE

a	wave amplitude
d	still water depth
$\boldsymbol{f} = (f_x, f_y, f_z)$	force per unit length
g	acceleration of gravity
H_s	significant wave height
k	wave number
L	wavelength
m_0	zeroth moment of the wave spectrum in deep water
N	number of periodic components with infinitesimal amplitudes
p	fluid pressure
R	radiation stress tensor
S	directional wave spectrum
S_D	set-down
S_U	set-up
t	time
T	wave period
$\boldsymbol{v} = (v_x, v_y, v_z)$	particle velocity
x	horizontal coordinate axis
y	horizontal coordinate axis
z	vertical coordinate axis with the origin at the mean water level
Δ	variation of the mean water level due to the wave motion
ΔW	mean variation of the water volume
ε	phase angle
η	surface displacement
ϑ	angle between the y-axis and the direction of wave advance
λ	seabed slope
ρ	fluid density
σ	r.m.s. surface displacement of a sea state
ϕ	velocity potential
ω	angular frequency

SUBSCRIPT

0	deep water
b	breaking
f	seabed
p	peak

SYMBOLS

$< f(t) >$	temporal mean
$\dot{F}$	derivative

1. INTRODUCTION

Waves dissipate most of their energy by breaking across surf zones as they approach land. However, a portion of this energy is partially converted into potential energy as run-up on the foreshore of the beach (Hunt, 1959). Wave run-up (i.e., the maximum level a wave reaches on the beach compared to the level of still-water) is often expressed in terms of a vertical excursion consisting of two components: (1) wave set-up (i.e., super elevation of the mean water level (MWL)), and (2) wave swash (i.e., fluctuations a`bout the MWL). Understanding wave run-up, set-up and related aspects of wave propagation are critical for predicting coastal risks and for planning and managing coastal protection strategies (Barbaro and Foti, 2013). For example, wave run-up is a primary cause of beach and dune erosion (Ruggiero *et al.*, 2001; Sallenger, 2000; Tomasicchio et al., 2011; Arena et al., 2013b), and set-up is related to catastrophic flooding in coastal areas.

Wave set-up was first observed scientifically in 1938 when hurricane waves raised mean water level at the shoreline by approximately 1 m (Fairchild 1958; Savage 1957; Saville 1961). From those initial observations, mathematical expressions have been proposed to approximate the movement of waves spilling and breaking (Longuet-Higgins, 1963) and to estimate wave height in relation to seabed slope (Bowen *et al.*, 1968). Others have found direct proportionality between wave set-up and significant wave height (Guza and Thornton, 1981) such that set-up is related to the ratio between significant wave height in deep water and on the slope of the beach (Nielsen, 1988, 1989). Furthermore, Holman and Sallenger (1985) have found a correlation between wave set-up and Iribarren number (Iribarren and Nielsen, 1949) defined as the ratio between the beach slope and the wave steepness, it is a measure for whether breaking would occur on a plane slope. However, Hanslow and Nielsen (1993) observed that wave set-up on dissipative beaches does not depend on beach slope, and, therefore, on Iribarren number. Finally, other research has investigated the relationship of offshore root-mean-square (RMS) wave height (King *et al*., 1990) and water depth (Lentz and Raubenheimer, 1999; Raubenheimer *et al*., 2001; Apotsos *et al*., 2007) on wave set-up.

Recently, Stockdon *et al.* (2006) proposed parameters for wave set-up, swash, and run-up where set-up at the shoreline assumed a dimensional form of the more common Irribarren-based expression (usually adopted for a plunging breaker) that includes foreshore beach slope, offshore wave height, and deep-water wavelength (Battjes, 1974 a,b). Massel and Pelinovsky (2001) showed that set-up affects remarkably also the run-up height by describing the set-up mechanism via the cross-shore balance of momentum. Their study neglected the permeability of the sea bottom. Longuet-Higgins (1983), Kang and Nielsen (1996), and Li and Barry (2000) have studied wave set-up in the case of a permeable ocean bottom.

In this study, following the logic of Longuet-Higgins (1963) for regular waves and Barbaro and Martino (2007), we derived a new expression for determining wave set-up for random, wind-generated sea waves in order to investigate the influence of directional spectrum (Boccotti et al., 2011) on wave set-up.

2. RADIATION STRESS, SET-DOWN AND SET-UP FOR RANDOM WAVES

2.1 RADIATION STRESS

We considered a Cartesian co-ordinate system x, y, z where the x-axis was along the shoreline, the y-axis was orthogonal to the x-axis and landward oriented, and the origin of the vertical z-axis was at MWL (Figure 1).

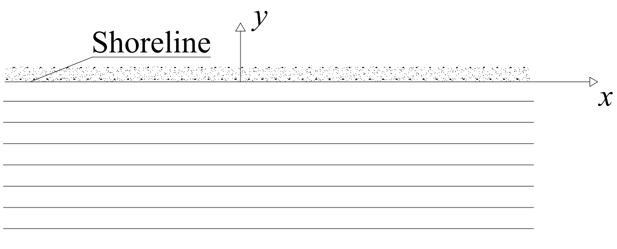

Figure 1. Cartesian co-ordinate system x, y, z where the x-axis was along the shoreline, the y-axis was orthogonal to the x-axis and landward oriented, and the origin of the vertical z-axis was at MWL.

This system assumed that contour lines were straight and parallel to the x-axis, the seabed was flat, fluid was inviscid, and flow was irrotational up to the breaker line. In this context, a velocity potential existed and could be approximated at the first order in a Stokes' expansion. By applying the sea states theory (Longuet-Higgins, 1963; Phillips, 1967; Borgman, 1972), we calculated the velocity potential as the sum of a large number (N) of periodic components with infinitesimal amplitudes (a_{i0}) and frequencies (ω_i) that were different from each other as well as random phase angles (ε_i) that were stochastically independent and uniformly distributed over the interval [0, 2π]. Thus, the system was a stationary Gaussian process that, assuming a three-dimensional domain, could be expressed by the equation:

$$\phi(x,y,z,t) = g\sum_{i=1}^{N} a_{i_0}\,\omega_i^{-1}\,\frac{\cosh\left[k_i\left(d+z\right)\right]}{\cosh\left(k_i\,d\right)}\,, \\ \times\sin\left(k_i\,x\sin\vartheta_{i_0} + k_i\,y\cos\vartheta_{i_0} - \omega_i\,t + \varepsilon_i\right) \tag{1}$$

where g was the acceleration due to gravity, and ϑ_{i0} was the angle that the propagation direction of the ith component made with the y-axis. Wave number (k_i) was the solution of the dispersion relation according to:

$$k_i\,\tanh\left(k_i d\right) = \omega_i^2 / g\,, \tag{2}$$

where d was water depth. Free surface displacement was given by:

$$\eta(x,y,t) = \sum_{i=1}^{N} a_{i_0}\cos\left(k_i\,x\sin\vartheta_{i_0} + k_i\,y\cos\vartheta_{i_0} - \omega_i\,t + \varepsilon_i\right) \tag{3}$$

with variance:

$$\sigma_0^2 = \int_0^{\infty}\int_0^{2\pi} S_0\left(\omega,\vartheta_0\right)\mathrm{d}\vartheta_0\,\mathrm{d}\omega\,, \tag{4}$$

where $S_0(\omega, \vartheta_0)$ was the directional spectrum of the surface displacement in deep water, defined as:

$$S_0\left(\omega,\vartheta_0\right)\delta\vartheta_0\,\delta\omega = \frac{1}{2}\sum_i a_{i_0}^2 \tag{5}$$

$$\text{for } i \text{ such that } \begin{cases}\omega < \omega_i < \omega + \delta\omega \\ \vartheta < \vartheta_{i_0} < \vartheta + d\vartheta\end{cases}.$$

According to Longuet-Higgins and Stewart (1964), radiation stress tensor components were defined as:

$$R_{yy}\left(y\right) = \lim_{T\to\infty}\frac{1}{T}\int_0^T\int_0^{\eta} p + \rho\,v_y^2\,\mathrm{d}z\,\mathrm{d}t \tag{6}$$

$$R_{xy}\left(y\right)=\lim_{T\to\infty}\frac{1}{T}\int_0^T\int_0^\eta v_x\, v_y\,\mathrm{d}z\,\mathrm{d}t\,, \tag{7}$$

where p was the fluid pressure, ρ was the fluid density, and v_x and v_y were the velocity components along the x-axis and y-axis, respectively. At the first order in a Stokes' expansion, velocity and wave pressure were related to velocity potential (Equation 1). Thus, radiation stress components can be given by the equation:

$$R_{yy}\left(y\right)=\frac{1}{2}\rho g\, d^2+ \\ +\frac{1}{2}\rho g\sum_{i=1}^{N}\frac{1}{2}a_i^2\left[\frac{2k_i\, d}{\sinh\left(2k_i\, d\right)}\left(1+\cos^2\vartheta_i\right)+\cos^2\vartheta_i\right] \tag{8}$$

$$R_{xy}\left(y\right)=\frac{1}{2}\rho g\sum_{i=1}^{N}\frac{1}{2}a_i^2\left[\frac{\sinh\left(2k_i\, d\right)+2k_i\, d}{\sinh\left(2k_i\, d\right)}\right]\sin\vartheta_i\cos\vartheta_i \tag{9}$$

Amplitudes (a_i) and directions (ϑ_i) were estimated at a fixed water depth (d).

2.2 SET-DOWN

Linear momentum in the y-direction was estimated from the control volume (Figure 2) extending from deep to shallow water according to the equation (Boccotti, 2000):

$$< f_{fy} > = -R_{yy}\left(y_1\right)+R_{yy}\left(y_2\right), \tag{10}$$

where $<f_{fy}>$ was the mean force per unit length exerted by the seabed. Because contour lines were parallel to the x-axis, $<f_{fy}>$ was therefore constant with respect to x.

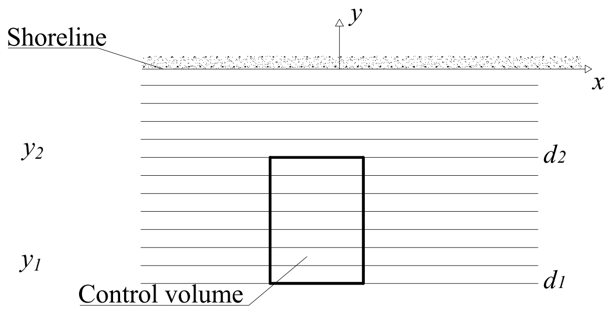

Figure 2. Control volume extending from y_1 (value of y-axis at deep water d_1) to y_2 (value of y-axis at shallow water d_2).

To be consistent with Equation 10, we applied second order variations to parameters for water depth such that $<f_{fy}>$ was related to variation in MWL (Δ) according to the equation:

$$< f_{fy} > = \int_{y_1}^{y_2}\rho\, g\left(d+\Delta\right)\frac{\mathrm{d}d}{\mathrm{d}y}\mathrm{d}y\,. \tag{11}$$

We rewrote Equation 10 by assuming that y_1 was associated with deep water, y_2 was associated with water depth d, and radiation stress was given by Equation 8. In this context, the linear momentum equation was given by:

$$\frac{\mathrm{d}\Delta}{\mathrm{d}d}=-\frac{1}{2}\frac{1}{d/L_{p_0}}\sum_{i=1}^{N}\frac{1}{2}a_{i_0}^2\frac{\mathrm{d}}{\mathrm{d}d}F_2\left(k_i\, d\right) \tag{12}$$

in which L_{p0} was the wavelength related to the dominant wave period in deep water and

$$F_2\left(k_i d\right)\equiv \\ \equiv\frac{\sinh\left(2k_i\, d\right)}{\tanh\left(k_i\, d\right)\left[\sinh\left(2k_i\, d\right)+2k_i\, d\right]} \\ \times\sqrt{\frac{1-\sin^2\vartheta_{i_0}}{1-\sin^2\vartheta_{i_0}/\tanh^2\left(k_i\, d\right)}} \\ \times\left\{\frac{2k_i\, d}{\sinh\left(2k_i\, d\right)}\left[2-\sin^2\vartheta_{i_0}\tanh^2\left(k_i\, d\right)\right]+1\right. \\ \left.-\sin^2\vartheta_{i_0}\tanh^2\left(k_i\, d\right)\right\}-\cos^2\vartheta_{i_0} \tag{13}$$

Equation 12 is restates in a non-dimensional form as,

$$\frac{d\left(\Delta/\sigma_0\right)}{d\left(d/L_{p_0}\right)}=-\frac{\sigma_0/L_{p_0}}{2\left(d/L_{p_0}\right)^2} \\ \times\frac{\int_0^\infty\int_0^{2\pi}S_0\left(\omega,\vartheta_0\right)\left(k\, d\right)\dot{F}_2\left(kd\right)\frac{\sinh\left(2k\, d\right)}{\sinh\left(2k\, d\right)+2k\, d}\, d\vartheta_0\, d\omega}{\int_0^\infty\int_0^{2\pi}S_0\left(\omega,\vartheta_0\right)d\vartheta_0\, d\omega} \tag{14}$$

where $\dot{F}_2\left(kd\right)$ was the derivative of $F_2(kd)$ with respect to kd. We used Equation 14 to estimate variation in MWL, assuming that MWL was zero at infinite water depths. Finally, we considered wave set-down as the value of Δ at fixed breaking conditions or depths.

2.3 SHOALING-REFRACTION OF RANDOM WAVES

When we consider a point in intermediate or shallow water ($d > 0.5L_{p0}$), free surface displacement can be given by Equation 3, assuming k_i satisfies the linear dispersion rule given in Equation 2.

For a single wave component, a_{i0} over water depth d is related to a_i in deep water according to the shoaling-refraction law:

$$a_i = a_{i_0} \times \sqrt{\frac{\sinh(2k_i d)}{\tanh(k_i d)[\sinh(2k_i d)+2k_i d]} \frac{\cos(\vartheta_{i_0})}{\sqrt{1-\sin^2(\vartheta_{i_0})\tanh^2(k_i d)}}} \tag{15}$$

where wave direction in deep water (ϑ_{i0}) was related to wave direction over water depth d (ϑ_i) according to the Snell law:

$$\sin\vartheta_i = \sin\vartheta_{i_0} \tanh(k_i d). \tag{16}$$

Free surface displacement over water depth d can then be rewritten as:

$$\eta(x,y,t) = \sum_{i=1}^{N} a_i \times \sqrt{\frac{\sinh(2k_i d)}{\tanh(k_i d)[\sinh(2k_i d)+2k_i d]} \frac{\cos(\vartheta_{i_0})}{\sqrt{1-\sin^2(\vartheta_{i_0})\tanh^2(k_i d)}}} \times\cos\begin{pmatrix} k_i x \sin\vartheta_{i_0} \tanh(k_i d) + \\ +k_i y\sqrt{1-\sin^2(\vartheta_{i_0})\tanh^2(k_i d)} - \omega_i t + \varepsilon_i \end{pmatrix} \tag{17}$$

The ratio between the standard deviation of $\eta(x, y, t)$ and the standard deviation in deep water (equal to $m_0^{1/2}$ with m_0 being the zeroth moment of the wave spectrum in deep water) was equal to the ratio between significant wave height H_s at water depth d and significant wave height H_{s0} in deep water:

$$\frac{H_s}{H_{s_0}} = \sqrt{\frac{\left\{\int_0^\infty\int_0^{2\pi} S_0(\omega,\vartheta_0)\frac{\sinh(2kd)}{\tanh(kd)[\sinh(2kd)+2kd]} \times\frac{\cos(\vartheta_0)}{\sqrt{1-\sin^2(\vartheta_0)\tanh^2(kd)}}d\vartheta_0 d\omega\right\}}{\int_0^\infty\int_0^{2\pi} S_0(\omega,\vartheta_0)\,d\vartheta_0\,d\omega}} \tag{18}$$

The random waves propagates to the shoreline up to a certain water depth, as the wave breaking occurs. For identifying such a depth d_b (known as breaking depth), the following breaking criteria proposed by Kamphuis (1991) are exploited

$$\frac{H_{sb}}{d_b} = 0.56\exp(3.5\lambda), \tag{19}$$

$$H_{sb} = 0.095\exp(4\lambda)L_{bp}\tanh\left(\frac{2\pi d_b}{L_{bp}}\right), \tag{20}$$

where L_{bp} is the wavelength related to the dominant wave period at water depth d_b, and λ is the beach slope.

Criteria (19) and (20) pertain to a plunging breaker and to a spilling breaker type, respectively.

2.4 SET-UP

Figure 3 shows the control volume, delimited by parallel vertical lines, that extended from the breaking line to the shoreline. If we assume that λ is seabed slope and that the y-component of the average shear stress exerted by the seabed is null (commonly assumed for spilling breakers; Longuet-Higgins, 1971), then linear momentum can be given by the equation:

$$< f_{fy} > = -\frac{1}{2}\rho g d_b^2 - \tan\lambda\,\rho g < \Delta W >, \tag{21}$$

where $\rho <\Delta W>$ is the mean variation of water mass per unit length of the volume given in Figure 4.

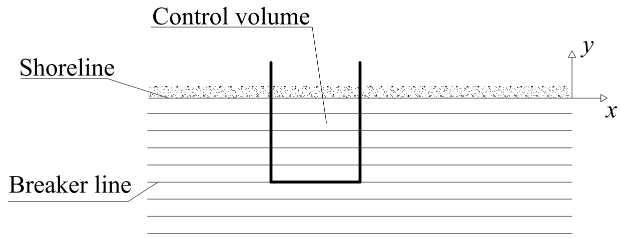

Figure 3. Control volume extending from the breaker line to the shoreline

Here, water depth at breaking is d_b-S_D, and mean force per unit length can be given by the equation:

$$< f_{fy} > = -\frac{1}{2}\rho g d_b^2 + \rho g d_b S_D - \frac{1}{2}\rho g \sum_{i=1}^{N}\frac{1}{2}a_{i_b}^2\left[\frac{2kd}{\sinh(2kd)}\left(1+\cos^2\vartheta_{i_b}\right)+\cos^2\vartheta_{i_b}\right] \tag{22}$$

Figure 4 depicts a cross section of a beach under these assumptions. In our framework, mean variation in water mass per unit length can be expressed is terms of wave set-up (S_U), which is defined as the super-elevation of the point of intersection between the mean water surface level and shore:

$$< \Delta W > = \frac{1}{2}(d_b - S_D)(d_b + S_U)\cot\lambda - \frac{1}{2}d_b^2\cot\lambda \tag{23}$$

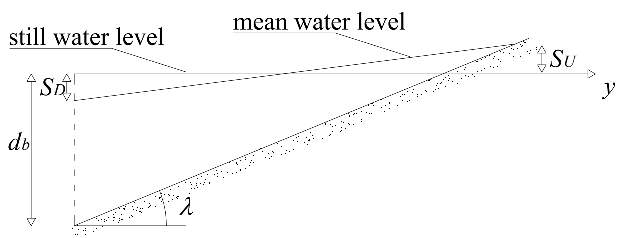

Figure 4. Cross-section of a beach. Wave set-up (S_U) is the super-elevation of the point of intersection between the mean water level and the shore above the still water level. Wave set-down (S_D) is the under-elevation of the

mean water level from the still water level at the depth d_b.

We then substituted Equations 22 and 23 into Equation 21 so that random wave set-up can be determined according to the equation:

$$S_U = -\frac{d_b S_D}{d_b - S_D} + \\ + \frac{1}{2(d_b - S_D)} \sum_{i=1}^{N} \frac{1}{2} a_{i_b}^2 \left[\frac{2 k_i d_b}{\sinh(2 k_i d_b)} \left(1 + \cos^2 \vartheta_{i_b}\right) + \cos^2 \vartheta_{i_b} \right] \tag{24}$$

For convenience, we expressed this relationship in a non-dimensional form and related it to the wave spectrum at infinite water depths:

$$\frac{S_u}{\sigma_0} = -\frac{S_D/\sigma_0}{1 - \frac{S_D}{\sigma_0}\frac{L_{p0}}{d_b}\frac{\sigma_0}{L_{p_0}}} + \\ + \frac{1/2}{\frac{d_b}{L_{p_0}}\frac{L_{p0}}{\sigma_0} - \frac{S_D}{\sigma_0}} \frac{1}{\int_0^\infty \int_0^{2\pi} S_0(\omega, \vartheta_0)\, d\vartheta_0\, d\omega} \left\{ \int_0^\infty \int_0^{2\pi} S_0(\omega, \vartheta_0) \right. \\ \times \frac{\sinh(2kd)}{\tanh(kd)\left[\sinh(2kd) + 2kd\right]} \sqrt{\frac{1 - \sin^2 \vartheta_0}{1 - \sin^2 \vartheta_0 \tanh^2(kd)}} \\ \times \left[\frac{2kd}{\sinh(2kd)} \left(2 - \sin^2 \vartheta_0 \tanh^2(kd)\right) + \right. \\ \left. \left. + 1 - \sin^2 \vartheta_0 \tanh^2(kd) \right] d\vartheta_0\, d\omega \right\} \tag{25}$$

3. APPLICATION

3.1 DATA AND PRELIMINARY CALCULATIONS

Wave set-up was calculated from buoy data collected at locations in Italy (Istituto Superiore per la Protezione e la Ricerca Ambientale; Figure 5) and the United States (National Data Buoy Center; Figure 6). Locations were chosen for the availability of data related to significant wave height and dominant wave direction (Table 1), as adequate data are needed for a reliable estimate of the wave climate (Arena et al., 2013a; Barbaro, 2011).

Significant wave height and dominant wave direction have previously been used to estimate the frequency of occurrence of a sea state in which the significant wave height was in a given interval and the dominant direction was in a given sector (each sector has an amplitude of 15°). Using this information, the weighted mean of the significant wave height for each sector was determined.

Figure 5. Location of buoys off of the Italian coast.

Figure 6. Location of buoys off of the coast of the United States.

Table 1. Time interval and record of sea states for each buoy location.

Location	Database	Time interval		Record of sea states
		Beginning	End	
Alghero	ISPRA	1/7/1989 0:00	5/4/2008 7:00	110.775
Cetraro	ISPRA	1/1/1999 0:00	5/4/2008 7:00	90.796
Crotone	ISPRA	1/7/1989 0:00	15/7/2007 20:30	111.423
Mazara del Vallo	ISPRA	1/7/1989 0:00	4/4/2008 22:00	106.262
Ortona	ISPRA	1/7/1989 0:00	24/3/2008 5:00	93.499
Florida	NDBC (42003)	1/1/1991 0:00	31/12/2009 23:00	104.246
California	NDBC (46042)	1/1/1995 0:00	31/12/2009 23:00	147.305

3.2 INFLUENCE OF THE DIRECTIONAL SPECTRUM ON THE SET-UP

Set-up, set-down and water depth at breaking were calculated using significant wave height and offshore directional wave spectrum for each sector in the study area. Directional spectrum was defined by (1) a frequency spectrum (e.g., Pierson-Moskowitz (Pierson and Moskowitz, 1964), JONSWAP (Hasselmann *et al.*, 1973) and Ochi-Hubble (Ochi and Hubble, 1976)) and (2) a spreading function (e.g, cosine-power (Mitsuyasu *et al.*, 1975), hyperbolic spreading function (Donelan *et al.*, 1985)). Further, the breaking conditions (19)-(20) are utilized by assuming the constant slope λ=0.035.

Using different combinations of frequency and spreading functions, we estimated a range of values for wave set-up (Figure 7). For example, the maximum estimated set-up, assuming the Ochi-Hubble spectrum and the cosine-power spreading function, was 0.19 m for the study location at Alghero. In general, use of the Ochi-Hubble directional spectrum resulted in the largest set-up estimate in all study sectors.

Set-up values differed by 5% when assuming cosine-power and hyperbolic spreading functions (assuming either JONSWAP and Pierson-Moskowitz frequency spectra). In addition, this percentage difference varied depending on the dominant direction with respect to the *y*-axis; the difference was 12% for the oblique dominant direction and less than 2% for orthogonal dominant direction. We observed the same behaviour assuming the Ochi-Hubble spectrum; however, the range in percentage difference decreased to 1% (mean difference) and 2% (oblique dominant direction).

Set-up was most influenced by the assumed frequency spectrum. Under fixed spreading functions, the Ochi-Hubble spectrum resulted in the largest set-up values while the JONSWAP spectrum resulted in the smallest.

For example, at the Alghero study location, we found that the mean ratio in wave set-up estimate was 2.8 assuming a Ochi-Hubble spectrum versus a JONSWAP spectrum. The same ratio between a Ochi-Hubble spectrum and a Pierson-Moskowitz spectrum was 2.6. In general, a wider the spectrum resulted in larger set-up estimates. We observed similar patterns at other study locations under study the conclusions drawn(Table 2). The largest set-up value was estimated for California. In Italy, the largest value was estimated for Alghero, where the highest waves on the Italian coastline have been recorded (Arena and Barbaro, 1999), and the smallest values were estimated for Ortona.

Tables 3 show the sector of wave propagation, the significant wave height, and the calculated set-up, set-down and water depth at breaking in the locations under study. It is noteworthy that the maximum set-up corresponds to the maximum significant wave height.

The dominant direction influences the set-up as well. The more oblique the waves are, the smaller the set-up is.

Table 2: Maximum estimated wave set-up for each study location.

Location	**Maximum Set-up [m]**	**Sector [degree]**[1]
Alghero	0.19	-57.5
Cetraro	0.14	-10.5
Crotone	0.14	-47.5
Mazara del Vallo	0.15	-62.5
Ortona	0.12	-7.5
Florida	0.16	-28.5
California	0.21	-18.5

[1] Sector of the maximum set-up is defined by its mean angle (degree).

4. CONCLUSIONS

In this study, we introduced a mathematical function for estimating wave set-up for random waves. . This expression allows introducing the random nature of the sea waves into the set-up calculation. Thus, it relates to a more physical consistent description of the set-up phenomenon, if compared to classical solutions involving monochromatic waves. Using this new function, we also demonstrated that wave set-up was highly influenced by different types of sea state taking account of different frequency spectrum, with the highest estimates made under the Ochi-Hubble spectrum and the smallest under the JONSWAP spectrum. Set-up was also influenced by the assumed spreading function and dependent on the dominant direction (with respect to the *y*-axis). In general, for a given significant wave height, wave set-up is at its highest at higher significant wave heights and when the dominant direction is orthogonal to the shoreline.

5. REFERENCES

1. APOTSOS A, RAUBENHEIMER B, ELGAR S, GUZA R T and SMITH J A (2007) Effects of wave rollers and bottom stress on wave setup. *Journal of Geophysical Research* 112(C02003).
2. ARENA F and BARBARO G (1999) *Il rischio ondoso nei mari italiani*. Editoriale BIOS, Cosenza, Italy.
3. ARENA F, LAFACE V, BARBARO G and ROMOLO A (2013a) Effects of sampling between records for intensity and duration of severe sea storms. International Journal of Geosciences 4(1): 240–248.
4. ARENA F, MALARA G, BARBARO G, ROMOLO A and GHIRETTI S (2013b) Long-term modeling of wave run-up and overtopping

during sea-storms. Journal of Coastal Research 29(2) : 419–429.

5. BARBARO G (2011) Estimating design wave for offshore structures in Italian waters. Maritime Engineering 164: 115–125.
6. BARBARO G and FOTI G (2013) Shoreline behind a breakwater: comparison between theoretical models and field measurements for the Reggio Calabria sea. Journal of Coastal Research 29(1): 216–224.
7. BARBARO G and MARTINO M C (2007) A new expression of the set-up for random wind generated waves. *Proceedings of the 5th International Conference of Coastal Structures*. Venice, Italy, pp. 1794–1805.
8. BATTJES J A (1974) *Computation of set-up, longshore currents, run up and overtopping due to wind-generated waves*. Department of Civil Engineering, Delft University of Technology, Report 74, Delft, The Netherlands.
9. BATTJES J A (1974) Surf Similarity. *Proceedings of the 14th International Conference on Coastal Engineering*. Copenhagen, Denmark, pp. 466–480.
10. BOCCOTTI P (2000) *Wave mechanics for ocean engineering*. Elsevier Oceanography Series, Oxford, United Kingdom.
11. BOCCOTTI P, ARENA F, FIAMMA V, ROMOLO A and BARBARO G (2011) Estimation of mean spectral directions in random seas. Ocean Engineering 38: 509–518.
12. BORGMAN L E (1972) Confidence intervals for ocean wave spectra. *Proceedings of the 13th International Conference on Coastal Engineering.* Vancouver, Canada, pp. 237–250.
13. BOWEN A J, INMAN DL and SIMMONS V P (1968) Wave 'set-down' and set-up. *Journal of Geophysical Research* 73(8): 2569–2577.
14. DONELAN M A, HAMILTON J and HUI W H (1985) Directional spectra of wind-generated waves. *Philosophical Transactions of the Royal Society of London A* 315(1534): 509–562.
15. FAIRCHILD J C (1958) *Model study of wave set-up induced by hurricane waves at Narragansett Pier, Rhode Island*. Bulletin of the Beach Erosion Board, U.S. Army Corps of Engineers, Washington, DC.
16. GUZA R T and THORNTON E B (1981) Wave set-up on a natural beach. *Journal of Geophysical Research* 86(C5): 4133–4137.
17. HANSLOW D and NIELSEN P (1993) Shoreline set-up on natural beaches. *Journal of Coastal Research* 15: 1–10.
18. HASSELMANN K, BARNETT T P, BOUWS E, CARLSON H, CARTWRIGHT D E, ENKE K, EWING J A, GIENAPP H, HASSELMANN DE, KRUSEMAN P, MEERBURG A, MULLER P, OLBERS DJ, RICHTER K, SELL W, and WALDEN H (1973) *Measurements of wind wave growth and swell decay during the Joint North Sea Wave Project (JONSWAP)*. Deutches Hydrographisches Institut, Hamburg, Germany.
19. HOLMAN R A and SALLENGER A H Jr (1985) Setup and swash on a natural beach. *Journal of Geophysical Research* 90(C1): 945–953.
20. HUNT I A (1959) Design of seawalls and breakwaters. *Journal of Waterways and Harbours Division* 85: 123–152.
21. IRIBARREN CR and NOGALES C (1949) Protection des ports. Proceedings of the 17th International Navigation Congress, Section 2. Lisbon, Portugal, pp. 31–80.
22. KANG HY and NIELSEN P (1996) Watertable dynamics in coastal areas. Proceedings of 25th International Conference on Coastal Engineering. Orlando, Florida, USA, 3: pp. 4601–4612.
23. KING B A, BLACKLEY M W L, CARR A P and HARDCASTLE P J (1990) Observations of wave-induced set-up on a natural beach. *Journal of Geophysical Research* 95(C12): 22289–22297.
24. LENTZ S and RAUBENHEIMER B (1999) Field observations of wave setup. *Journal of Geophysical Research* 104(C11): 25867–25875.
25. LI L and BARRY D A (2000) Wave-induced beach groundwater flow. *Advances in Water Research* 23(4): 325–337.
26. LONGUET-HIGGINS M S (1963) The effects of non- linearities on statistical distributions in the theory of sea waves. *Journal of Fluid Mechanics* 17(3): 459–480.
27. LONGUET-HIGGINS M S (1971) *Recent progress in the study of longshore currents*. Waves on beaches and resulting sediment transport, Proceedings of an advanced seminar conducted by the Mathematics Research Center, University of Wisconsin, USA, and the Coastal Engineering Research Center, U.S. Army Corps of Engineers, Washington, DC, USA.
28. LONGUET-HIGGINS M S (1983) Wave set-up, percolation and undertow in the surf zone. *Proceedings of the Royal Society of London A* 390(1799): 283–291.
29. LONGUET-HIGGINS M S and STEWART R W (1962) Radiation stress and mass transport in gravity waves, with application to 'surf-beats'. *Journal of Fluid Mechanics* **13(4)**: 481–504.
30. LONGUET-HIGGINS M S and STEWART R W (1964) Radiation stress in water waves: a physical discussion with applications. *Deep-Sea Research* **11(4)**: 529–562.
31. MASSEL S.R., PELINOVSKY E.N. (2001) Run-up of dispersive and breaking waves on beaches. Oceanologia 43: 61–97.

32. MITSUYASU H, TASAI F, SUHARA T, MIZUNO S, OHKUSO M, HONDA T and RIKIISHI K (1975) Observations of the directional spectrum of ocean waves using a cloverleaf buoy. *Journal of Physical Oceanography* 5(4): 750–760.
33. NIELSEN P (1988) Wave setup: A field study. *Journal of Geophysical Research* 93(C12): 15643–15652.
34. NIELSEN P (1989) Wave setup and runup: An integrated approach. *Coastal Engineering* 13(1): 1–9.
35. OCHI M K and HUBBLE E N (1976) Six-parameter wave spectra. *Proceedings of the 15th International Conference on Coastal Engineering*. Honolulu, Hawaii, USA, pp. 301–328.
36. PHILLIPS O M (1967) The theory of wind-generated waves. *Advances in Hydroscience* **4**: 119–149.
37. PIERSON W J Jr. and MOSKOWITZ L (1964) A proposed spectral form for fully developed wind seas based on the similarity theory of S.A. Kitaigorodskii. *Journal of Geophysical Research* 69(24), 5181–5190.
38. RAUBENHEIMER B, GUZA RT and ELGAR S (2001) Field observations of wave-driven setdown and setup. *Journal of Geophysical Research* 106(C23): 4629–4638.
39. RUGGIERO P, KOMAR P D, MCDOUGAL W G, MARRA J J and BEACH R A (2001) Wave runup, extreme water levels and the erosion of properties backing beaches. *Journal of Coastal Research* 17(2): 407–419.
40. SALLENGER A H (2000) Storm impact scale for barrier islands. *Journal of Coastal Research* 16(3): 890–895.
41. SAVAGE R P (1957) *Model tests for hurricane protection project*. Bulletin of the Beach Erosion Board, U.S. Army Corps of Engineers, Washington, DC.
42. SAVILLE T J (1961) Experimental determination of wave set-up. *Proceedings of 2nd Technical Conference on Hurricanes*. Miami Beach, Florida, USA, pp. 242–252.
43. STOCKDON H F, HOLMAN R A, HOWD P A and SALLEGER A H (2006) Empirical parameterization of setup, swash, and runup. *Coastal Engineering* 53: 573–588.
44. TOMASICCHIO GR, D'ALESSANDRO F and BARBARO G (2011) Composite modelling for large-scale experiments on wave-dune interaction. Journal of Hydraulic Research 49(S1): 15–19.

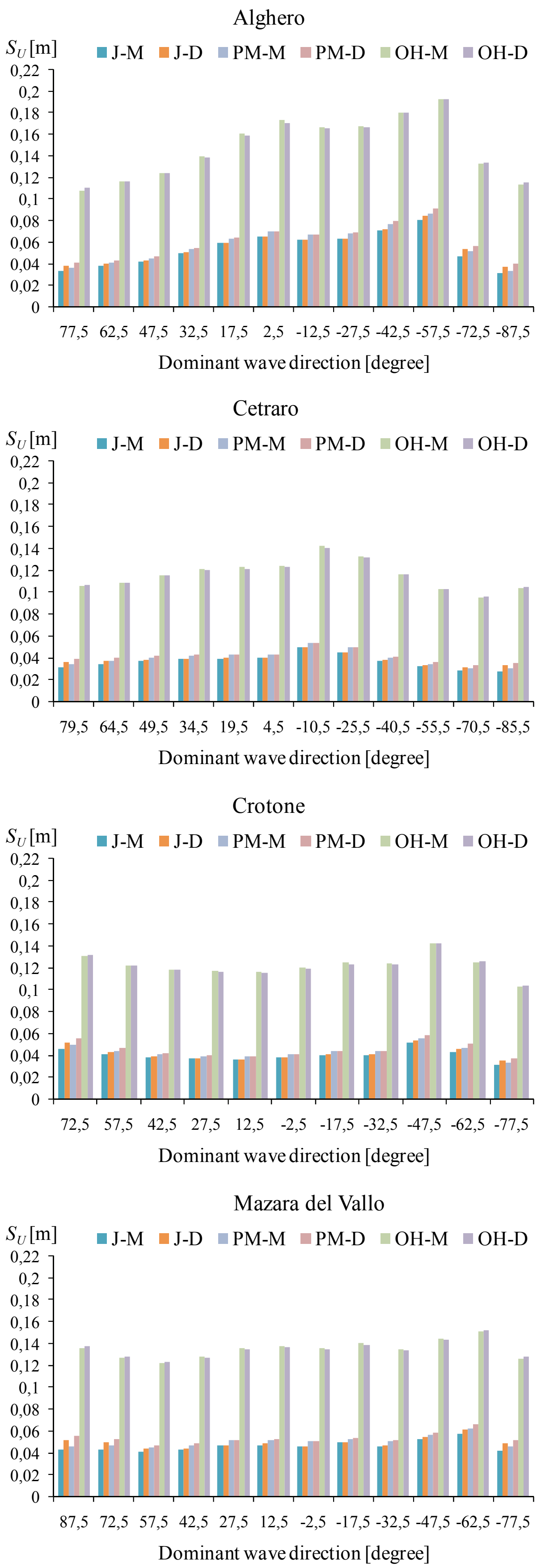

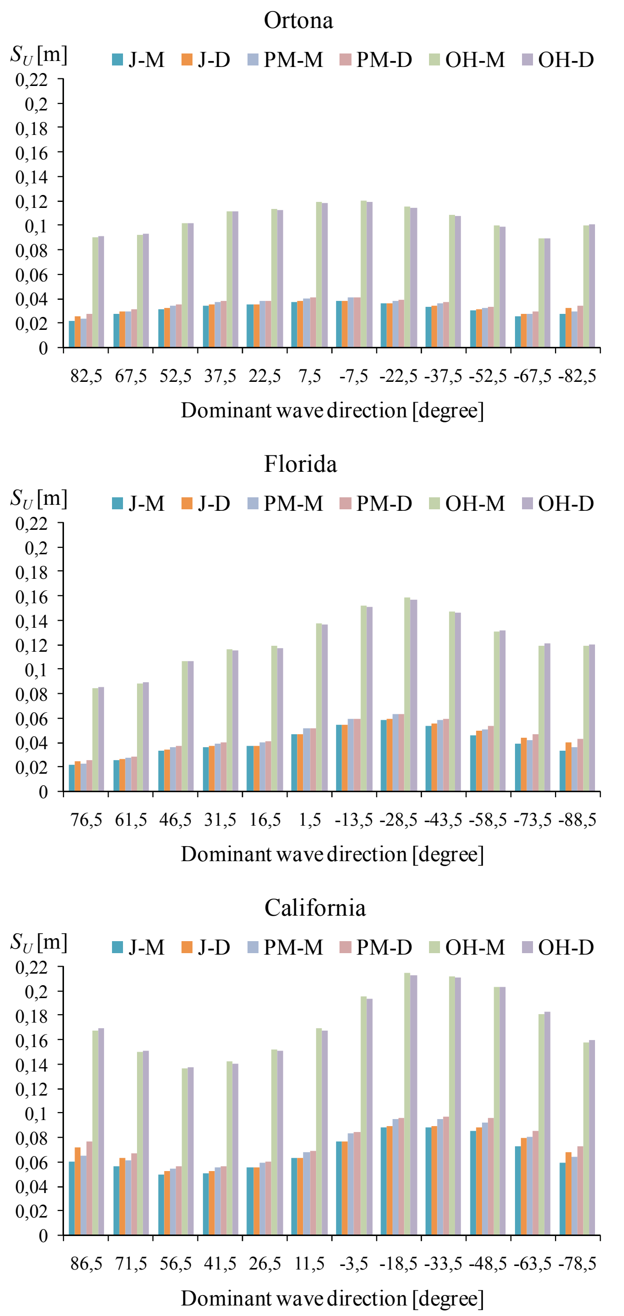

Figure 7. Set-up determined for each location by assuming a combination of frequency spectrum (Pierson-Moskowitz (PM), JONSWAP (J) and Ochi-Hubble (OH)) and spreading function (Mitsuyasu et al. (M) and Donelan et al. (D)).

						Alghero						
Sector [°]	**172.5**	**187.5**	**202.5**	**217.5**	**232.5**	**247.5**	**262.5**	**277.5**	**292.5**	**307.5**	**322.5**	**337.5**
H_s [m]	1.22	1.19	1.17	1.27	1.45	1.57	1.51	1.60	1.93	2.41	1.63	1.21
d_b J [m]	1.7	1.85	2	2.33	2.78	3.07	2.92	2.99	3.39	3.86	2.36	1.58
d_b J-D [m]	1.39	1.69	1.93	2.3	2.76	3.05	2.9	2.96	3.31	3.63	2.01	1.15
d_b PM [m]	1.74	1.84	1.97	2.29	2.73	3	2.87	2.94	3.34	3.85	2.39	1.63
d_b PM-D [m]	1.43	1.69	1.9	2.26	2.71	2.99	2.85	2.91	3.25	3.6	2.05	1.19
d_b OH [m]	1.16	1.38	1.56	1.82	2.13	2.32	2.22	2.25	2.46	2.65	1.59	0.96
d_b OH-D [m]	1.17	1.38	1.56	1.82	2.12	2.31	2.21	2.24	2.46	2.66	1.6	0.98
S_uJ [m]	0.033	0.038	0.042	0.049	0.059	0.065	0.062	0.063	0.071	0.08	0.047	0.031
S_uJ-D [m]	0.038	0.04	0.043	0.05	0.059	0.065	0.062	0.063	0.072	0.084	0.053	0.037
S_uPM [m]	0.036	0.041	0.045	0.053	0.063	0.07	0.067	0.068	0.077	0.086	0.051	0.033
S_uPM-D [m]	0.041	0.043	0.047	0.054	0.064	0.07	0.067	0.069	0.079	0.091	0.056	0.04
S_uOH [m]	0.108	0.116	0.124	0.14	0.161	0.173	0.167	0.168	0.18	0.193	0.133	0.113
S_uOH-D [m]	0.11	0.116	0.124	0.139	0.159	0.171	0.166	0.167	0.18	0.193	0.134	0.115
S_d J [m]	-0.011	-0.011	-0.011	-0.013	-0.015	-0.016	-0.015	-0.016	-0.019	-0.023	-0.015	-0.013
S_d J-D [m]	-0.014	-0.012	-0.012	-0.013	-0.015	-0.016	-0.016	-0.016	-0.02	-0.024	-0.017	-0.017
S_d PM [m]	-0.013	-0.012	-0.013	-0.014	-0.017	-0.018	-0.017	-0.018	-0.021	-0.025	-0.017	-0.015
S_d PM-D [m]	-0.015	-0.014	-0.013	-0.015	-0.017	-0.018	-0.018	-0.018	-0.022	-0.027	-0.019	-0.018
S_d OH [m]	-0.056	-0.05	-0.05	-0.053	-0.058	-0.06	-0.059	-0.06	-0.064	-0.069	-0.059	-0.075
S_d OH-D [m]	-0.058	-0.051	-0.05	-0.053	-0.058	-0.06	-0.059	-0.06	-0.064	-0.07	-0.06	-0.075
						Cetraro						
Sector [°]	**157.5**	**172.5**	**187.5**	**202.5**	**217.5**	**232.5**	**247.5**	**262.5**	**277.5**	**292.5**	**307.5**	**322.5**
H_s [m]	1.17	1.11	1.05	1.02	0.98	0.97	1.20	1.14	1.00	0.94	0.94	1.06
d_b J [m]	1.62	1.7	1.77	1.86	1.87	1.89	2.33	2.14	1.78	1.53	1.38	1.4
d_b J-D [m]	1.29	1.54	1.7	1.83	1.86	1.88	2.31	2.12	1.74	1.44	1.19	1.04
d_b PM [m]	1.65	1.7	1.75	1.83	1.84	1.85	2.28	2.11	1.75	1.52	1.39	1.45
d_b PM-D [m]	1.32	1.54	1.68	1.8	1.82	1.85	2.27	2.08	1.7	1.43	1.21	1.08
d_b OH [m]	1.08	1.27	1.4	1.5	1.53	1.56	1.85	1.71	1.43	1.22	1.03	0.89
d_b OH-D [m]	1.1	1.28	1.4	1.5	1.53	1.55	1.84	1.7	1.43	1.22	1.04	0.91
S_uJ [m]	0.031	0.034	0.037	0.039	0.039	0.04	0.049	0.045	0.037	0.032	0.028	0.027
S_uJ-D [m]	0.036	0.037	0.038	0.039	0.04	0.04	0.049	0.045	0.038	0.033	0.031	0.033
S_uPM [m]	0.034	0.037	0.04	0.042	0.043	0.043	0.053	0.049	0.04	0.034	0.03	0.03
S_uPM-D [m]	0.039	0.04	0.042	0.043	0.043	0.043	0.053	0.049	0.041	0.036	0.033	0.035
S_uOH [m]	0.106	0.109	0.115	0.121	0.123	0.124	0.142	0.133	0.116	0.103	0.095	0.104
S_uOH-D [m]	0.107	0.109	0.115	0.12	0.121	0.123	0.141	0.132	0.116	0.103	0.096	0.105
S_d J [m]	-0.011	-0.01	-0.01	-0.01	-0.01	-0.01	-0.012	-0.012	-0.01	-0.009	-0.009	-0.011
S_d J-D [m]	-0.013	-0.011	-0.011	-0.01	-0.01	-0.01	-0.012	-0.012	-0.01	-0.01	-0.01	-0.014
S_d PM [m]	-0.013	-0.011	-0.011	-0.011	-0.011	-0.011	-0.014	-0.013	-0.011	-0.01	-0.01	-0.012
S_d PM-D [m]	-0.015	-0.013	-0.012	-0.012	-0.011	-0.011	-0.014	-0.013	-0.011	-0.011	-0.011	-0.015
S_d OH [m]	-0.058	-0.049	-0.048	-0.049	-0.049	-0.049	-0.053	-0.051	-0.048	-0.046	-0.048	-0.067
S_d OH-D [m]	-0.059	-0.05	-0.048	-0.048	-0.048	-0.049	-0.053	-0.051	-0.048	-0.046	-0.048	-0.068
						Crotone						
Sector [°]	**352.5**	**7.5**	**22.5**	**37.5**	**52.5**	**67.5**	**82.5**	**97.5**	**112.5**	**127.5**	**142.5**	**157.5**
H_s [m]	1.60	1.59	1.24	1.04	0.93	0.88	0.92	1.00	1.05	1.44	1.36	1.12
d_b J [m]	2.09	2.3	1.99	1.83	1.74	1.7	1.8	1.92	1.93	2.46	2.11	1.57
d_b J-D [m]	1.51	1.96	1.87	1.78	1.72	1.69	1.78	1.9	1.9	2.38	1.93	1.28
d_b PM [m]	2.16	2.33	1.98	1.8	1.71	1.67	1.76	1.88	1.9	2.43	2.11	1.6
d_b PM-D [m]	1.57	2	1.85	1.75	1.69	1.66	1.75	1.87	1.87	2.34	1.93	1.31
d_b OH [m]	1.21	1.55	1.5	1.46	1.43	1.42	1.49	1.57	1.55	1.86	1.54	1.08
d_b OH-D [m]	1.23	1.57	1.51	1.46	1.42	1.41	1.48	1.56	1.55	1.86	1.55	1.09
S_uJ [m]	0.041	0.046	0.041	0.038	0.037	0.036	0.038	0.04	0.04	0.051	0.043	0.031
S_uJ-D [m]	0.049	0.051	0.043	0.039	0.037	0.036	0.038	0.041	0.041	0.053	0.046	0.035
S_uPM [m]	0.044	0.049	0.044	0.041	0.039	0.039	0.041	0.044	0.044	0.055	0.047	0.033
S_uPM-D [m]	0.053	0.055	0.047	0.042	0.04	0.039	0.041	0.044	0.044	0.058	0.05	0.037
S_uOH [m]	0.132	0.131	0.122	0.118	0.117	0.116	0.12	0.125	0.124	0.142	0.125	0.103
S_uOH-D [m]	0.134	0.132	0.122	0.118	0.116	0.115	0.119	0.123	0.123	0.142	0.126	0.104
S_d J [m]	-0.018	-0.015	-0.011	-0.01	-0.009	-0.009	-0.009	-0.01	-0.011	-0.014	-0.013	-0.011
S_d J-D [m]	-0.022	-0.017	-0.013	-0.011	-0.01	-0.009	-0.01	-0.01	-0.011	-0.015	-0.014	-0.012
S_d PM [m]	-0.019	-0.016	-0.013	-0.011	-0.011	-0.01	-0.011	-0.011	-0.012	-0.016	-0.014	-0.012
S_d PM-D [m]	-0.024	-0.019	-0.014	-0.012	-0.011	-0.01	-0.011	-0.012	-0.012	-0.016	-0.015	-0.014
S_d OH [m]	-0.082	-0.059	-0.051	-0.048	-0.048	-0.047	-0.048	-0.049	-0.049	-0.054	-0.053	-0.055
S_d OH-D [m]	-0.083	-0.06	-0.051	-0.048	-0.047	0.047	-0.048	-0.049	-0.049	-0.055	-0.053	-0.056
						Mazara del Vallo						
Sector [°]	**127.5**	**142.5**	**157.5**	**172.5**	**187.5**	**202.5**	**217.5**	**232.5**	**247.5**	**262.5**	**277.5**	**292.5**
H_s [m]	1.67	1.51	1.25	1.18	1.19	1.16	1.12	1.20	1.20	1.46	1.80	1.54
d_b J [m]	2.18	2.19	2	2.07	2.23	2.25	2.19	2.3	2.21	2.5	2.79	2.15
d_b J-D [m]	1.58	1.86	1.88	2.02	2.2	2.23	2.17	2.28	2.17	2.41	2.56	1.75
d_b PM [m]	2.25	2.21	1.99	2.04	2.19	2.2	2.14	2.26	2.17	2.46	2.79	2.19
d_b PM-D [m]	1.64	1.9	1.87	1.99	2.16	2.19	2.13	2.24	2.13	2.37	2.56	1.8
d_b OH [m]	1.25	1.48	1.51	1.63	1.76	1.79	1.76	1.83	1.74	1.88	1.96	1.4
d_b OH-D [m]	1.28	1.5	1.52	1.62	1.76	1.78	1.75	1.82	1.73	1.88	1.97	1.41
S_uJ [m]	0.043	0.043	0.041	0.043	0.047	0.047	0.046	0.049	0.046	0.052	0.057	0.042
S_uJ-D [m]	0.051	0.049	0.044	0.044	0.047	0.048	0.046	0.049	0.047	0.054	0.061	0.048
S_uPM [m]	0.046	0.047	0.045	0.047	0.051	0.051	0.05	0.052	0.05	0.056	0.062	0.046
S_uPM-D [m]	0.055	0.052	0.047	0.048	0.051	0.052	0.05	0.053	0.051	0.058	0.066	0.051
S_uOH [m]	0.136	0.127	0.122	0.128	0.136	0.138	0.136	0.141	0.135	0.144	0.151	0.126
S_uOH-D [m]	0.138	0.128	0.123	0.127	0.135	0.137	0.135	0.139	0.134	0.143	0.152	0.128
S_d J [m]	-0.018	-0.014	-0.012	-0.012	-0.012	-0.012	-0.011	-0.012	-0.012	-0.014	-0.017	-0.014
S_d J-D [m]	-0.023	-0.016	-0.013	-0.012	-0.012	-0.012	-0.012	-0.012	-0.012	-0.015	-0.018	-0.017
S_d PM [m]	-0.02	-0.016	-0.013	-0.013	-0.013	-0.013	-0.013	-0.014	-0.013	-0.016	-0.019	-0.016

S_d PM-D [m]	-0.025	-0.018	-0.014	-0.013	-0.014	-0.014	-0.013	-0.014	-0.014	-0.017	-0.02	-0.019
S_d OH [m]	-0.083	-0.058	-0.051	-0.051	-0.052	-0.052	-0.052	-0.053	-0.052	-0.055	-0.059	-0.062
S_d OH-D [m]	-0.084	-0.059	-0.051	-0.051	-0.052	-0.052	-0.051	-0.052	-0.052	-0.055	-0.06	-0.063
Ortona												
Sector [°]	**157.5**	**172.5**	**187.5**	**202.5**	**217.5**	**232.5**	**247.5**	**262.5**	**277.5**	**292.5**	**307.5**	**322.5**
H_s [m]	0.82	0.88	0.90	0.91	0.87	0.91	0.92	0.89	0.88	0.86	0.82	1.03
d_b J [m]	1.11	1.32	1.49	1.64	1.65	1.77	1.79	1.69	1.58	1.43	1.23	1.39
d_b J-D [m]	0.86	1.17	1.42	1.61	1.63	1.76	1.78	1.67	1.55	1.36	1.09	1.07
d_b PM [m]	1.14	1.33	1.48	1.61	1.62	1.74	1.76	1.66	1.56	1.41	1.24	1.43
d_b PM-D [m]	0.88	1.18	1.4	1.58	1.61	1.73	1.75	1.64	1.53	1.34	1.1	1.11
d_b OH [m]	0.76	1.02	1.21	1.34	1.37	1.47	1.48	1.4	1.31	1.17	0.96	0.92
d_b OH-D [m]	0.77	1.03	1.21	1.34	1.37	1.46	1.48	1.39	1.3	1.17	0.97	0.94
S_uJ [m]	0.021	0.027	0.031	0.034	0.035	0.037	0.038	0.036	0.033	0.03	0.025	0.027
S_uJ-D [m]	0.025	0.029	0.032	0.035	0.035	0.038	0.038	0.036	0.034	0.031	0.027	0.032
S_uPM [m]	0.023	0.029	0.034	0.037	0.038	0.04	0.041	0.038	0.036	0.032	0.027	0.029
S_uPM-D [m]	0.027	0.031	0.035	0.038	0.038	0.041	0.041	0.039	0.037	0.033	0.029	0.034
S_uOH [m]	0.09	0.092	0.102	0.111	0.113	0.119	0.12	0.115	0.109	0.1	0.089	0.1
S_uOH-D [m]	0.091	0.093	0.102	0.111	0.112	0.118	0.119	0.114	0.108	0.099	0.089	0.101
S_d J [m]	-0.008	-0.008	-0.009	-0.009	-0.009	-0.009	-0.009	-0.009	-0.009	-0.008	-0.008	-0.01
S_d J-D [m]	-0.01	-0.009	-0.009	-0.009	-0.009	-0.009	-0.01	-0.009	-0.009	-0.009	-0.008	-0.012
S_d PM [m]	-0.009	-0.009	-0.01	-0.01	-0.01	-0.01	-0.011	-0.01	-0.01	-0.009	-0.008	-0.011
S_d PM-D [m]	-0.011	-0.01	-0.01	-0.01	-0.01	-0.011	-0.011	-0.01	-0.01	-0.01	-0.009	-0.014
S_d OH [m]	-0.058	-0.046	-0.045	-0.047	-0.047	-0.048	-0.048	-0.047	-0.046	-0.044	-0.045	-0.06
S_d OH-D [m]	-0.059	-0.047	-0.045	-0.047	-0.047	-0.048	-0.048	-0.047	-0.046	-0.045	-0.046	-0.061
Florida												
Sector [°]	**187.5**	**202.5**	**217.5**	**232.5**	**247.5**	**262.5**	**277.5**	**292.5**	**307.5**	**322.5**	**337.5**	**352.5**
H_s [m]	0.75	0.77	0.92	0.94	0.92	1.14	1.33	1.48	1.46	1.41	1.38	1.29
d_b J [m]	1.06	1.2	1.58	1.73	1.77	2.23	2.57	2.76	2.55	2.25	1.99	1.68
d_b J-D [m]	0.87	1.11	1.53	1.71	1.75	2.21	2.55	2.73	2.48	2.1	1.68	1.2
d_b PM [m]	1.08	1.2	1.56	1.7	1.73	2.18	2.52	2.71	2.52	2.24	2.01	1.73
d_b PM-D [m]	0.89	1.11	1.5	1.68	1.72	2.17	2.51	2.68	2.44	2.09	1.71	1.24
d_b OH [m]	0.78	0.98	1.28	1.42	1.46	1.78	2	2.1	1.93	1.66	1.36	0.99
d_b OH-D [m]	0.79	0.98	1.28	1.41	1.46	1.77	1.99	2.09	1.93	1.67	1.37	1.01
S_uJ [m]	0.021	0.025	0.033	0.036	0.037	0.047	0.054	0.058	0.053	0.046	0.039	0.033
S_uJ-D [m]	0.024	0.026	0.034	0.037	0.037	0.047	0.054	0.059	0.055	0.049	0.044	0.04
S_uPM [m]	0.022	0.027	0.036	0.039	0.04	0.051	0.059	0.063	0.058	0.05	0.042	0.036
S_uPM-D [m]	0.025	0.028	0.037	0.04	0.041	0.051	0.059	0.063	0.059	0.053	0.047	0.043
S_uOH [m]	0.084	0.088	0.107	0.116	0.119	0.138	0.152	0.159	0.147	0.131	0.119	0.119
S_uOH-D [m]	0.085	0.089	0.107	0.115	0.117	0.137	0.151	0.157	0.146	0.132	0.121	0.12
S_d J [m]	-0.007	-0.007	-0.009	-0.009	-0.009	-0.012	-0.014	-0.015	-0.014	-0.013	-0.013	-0.014
S_d J-D [m]	-0.008	-0.008	-0.009	-0.01	-0.01	-0.012	-0.014	-0.015	-0.015	-0.014	-0.015	-0.018
S_d PM [m]	-0.008	-0.008	-0.01	-0.011	-0.011	-0.013	-0.015	-0.017	-0.016	-0.015	-0.014	-0.016
S_d PM-D [m]	-0.009	-0.009	-0.01	-0.011	-0.011	-0.013	-0.015	-0.017	-0.017	-0.016	-0.016	-0.02
S_d OH [m]	-0.05	-0.043	-0.046	-0.048	-0.048	-0.052	-0.056	-0.058	-0.055	-0.053	-0.056	-0.08
S_d OH-D [m]	-0.05	-0.044	-0.046	-0.047	-0.048	-0.052	-0.055	-0.057	-0.055	-0.054	-0.058	-0.08
California												
Sector [°]	**157.5**	**172.5**	**187.5**	**202.5**	**217.5**	**232.5**	**247.5**	**262.5**	**277.5**	**292.5**	**307.5**	**322.5**
H_s [m]	2.34	1.94	1.48	1.37	1.39	1.54	1.87	2.18	2.29	2.41	2.34	2.19
d_b J [m]	3.08	2.83	2.39	2.42	2.61	2.99	3.65	4.18	4.19	4.1	3.61	3.04
d_b J-D [m]	2.26	2.43	2.25	2.36	2.58	2.96	3.63	4.14	4.13	3.95	3.28	2.45
d_b PM [m]	3.17	2.86	2.38	2.38	2.56	2.93	3.58	4.1	4.12	4.05	3.61	3.1
d_b PM-D [m]	2.34	2.47	2.23	2.32	2.53	2.91	3.56	4.07	4.05	3.88	3.29	2.51
d_b OH [m]	1.7	1.87	1.77	1.86	2.01	2.27	2.7	3.01	2.99	2.86	2.42	1.86
d_b OH-D [m]	1.74	1.89	1.77	1.85	2	2.25	2.68	3	2.98	2.86	2.43	1.89
S_uJ [m]	0.06	0.056	0.049	0.05	0.055	0.063	0.077	0.088	0.088	0.085	0.073	0.059
S_uJ-D [m]	0.072	0.063	0.052	0.052	0.055	0.063	0.077	0.089	0.089	0.088	0.079	0.068
S_uPM [m]	0.065	0.061	0.054	0.055	0.059	0.068	0.083	0.095	0.095	0.092	0.08	0.064
S_uPM-D [m]	0.077	0.067	0.056	0.056	0.06	0.069	0.084	0.096	0.097	0.096	0.085	0.073
S_uOH [m]	0.168	0.15	0.137	0.142	0.152	0.17	0.196	0.215	0.212	0.204	0.181	0.158
S_uOH-D [m]	0.17	0.151	0.138	0.141	0.151	0.168	0.194	0.213	0.211	0.204	0.183	0.16
S_d J [m]	-0.025	-0.018	-0.014	-0.014	-0.014	-0.016	-0.019	-0.022	-0.023	-0.023	-0.022	-0.021
S_d J-D [m]	-0.031	-0.02	-0.015	-0.014	-0.014	-0.016	-0.019	-0.023	-0.023	-0.024	-0.024	-0.025
S_d PM [m]	-0.028	-0.02	-0.016	-0.015	-0.016	-0.018	-0.022	-0.025	-0.026	-0.026	-0.024	-0.023
S_d PM-D [m]	-0.034	-0.022	-0.017	-0.016	-0.016	-0.018	-0.022	-0.025	-0.026	-0.027	-0.026	-0.027
S_d OH [m]	-0.093	-0.063	-0.054	-0.054	-0.056	0.06	-0.066	-0.071	-0.071	-0.07	-0.068	-0.073
S_d OH-D [m]	-0.094	-0.065	-0.055	-0.054	-0.056	-0.059	-0.065	-0.07	-0.071	-0.071	-0.069	-0.074